# A Method and Algorithm for Adaptive Equalization of Gamma Spectra Obtained from Small Scintillation Crystals

Bernd Laquai, 24.10.23

With the availability of small but highly efficient silicon photomultipliers (SiPM), manufacturers of equipment and modules for gamma radiation measurement and detection are increasingly making use of small scintillation crystals or crystal arrays to create small and cost-efficient detector units. These detector units are used for various advanced portable applications, but also highly complex imaging systems such as PET and SPECT or applications used in space exploration. The crystal material such as CsI, LSO/LYSO or BGO also shows an excellent efficiency for the conversion of photons into light pulses with a wavelength matched to the sensitivity of the silicon photo multiplier cells. However, when geometries of the scintillation crystals become very small, the overall photopeak efficiency curve shows a massive drop for higher photon energies and a sharp drop towards very low energies in response to a gamma radiation field with a broadband energy distribution (see fig. 1 and 2). On one hand this effect strongly attenuates the peak counting efficiency towards the high energies for small crystals. The reason for this distortion is the fact that the probability of contribution to the photopeak decreases with the crystal dimensions, since an incident photon may leave the crystal before all its energy is transferred to the crystal atoms, even for lower energy. On the other hand, the small detector units containing crystal and photo multiplier need to be protected against ambient light, humidity and mechanical stress which requires shielding materials that particularly absorb the very low energy photons and X-rays. This strongly attenuates the peak counting efficiency of a detector unit towards the very low energy side.

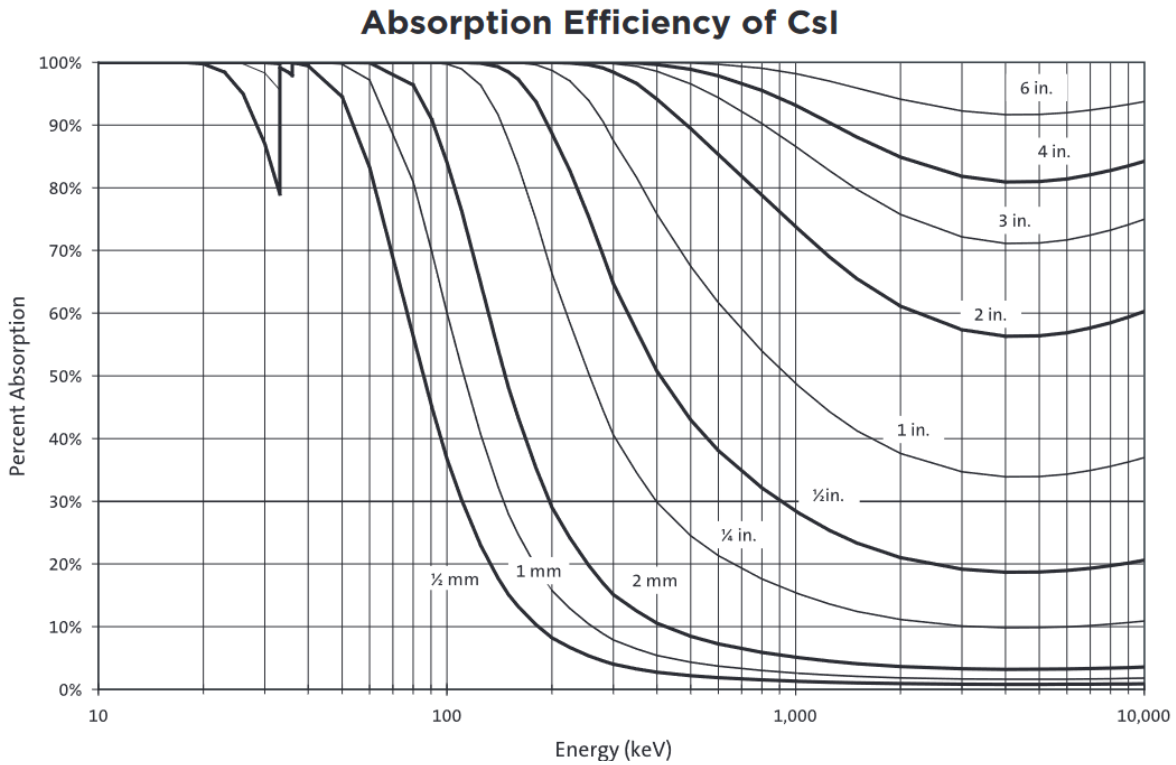


Fig. 1: Absorption efficiency of CsI crystals of different size according to /1/. For a crystal with 1.27mm (1/2in.) thickness only 30% of photons with 900keV energy will be absorbed.

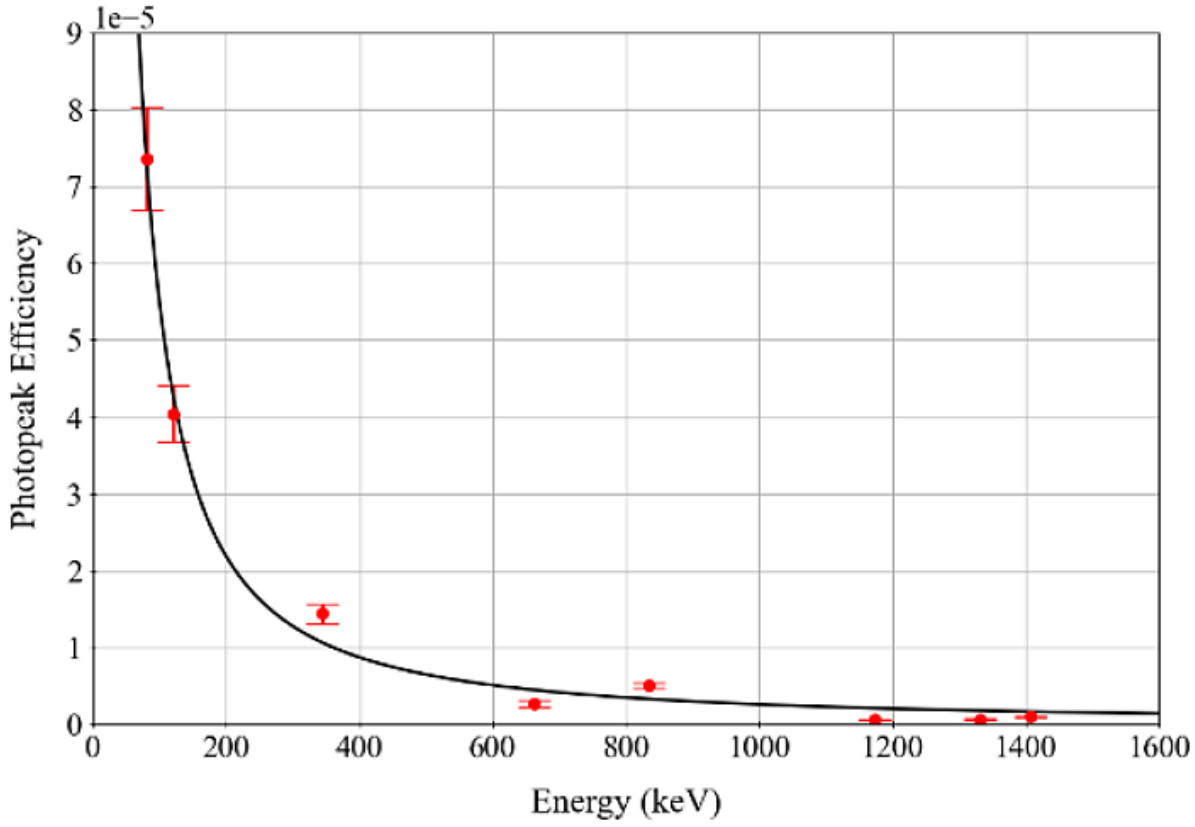


Fig. 2: Example of a fitted photopeak efficiency curve of a detector using a 6×6×15mm3 CsI(Tl) scintillator with SiPM. The graph shows the measurement results and modeling of the detector efficiency for energies > 80keV /2/

The impact of both attenuation effects quickly become visible when a small size handheld gamma measurement instrument such as the Radiacode RC-101 or RC-102, based on a 10x10x10mm CsI scintillation detector with SiPM /3/, is used to accumulate a spectrum of an old spark gap tube containing a blot of Cs137 for pre-ionization. Even with lead shielding and after 3 hours of spectrum accumulation the measurement result shows a strong spike located at about 80keV that outranges the expected photopeak of the Cs137 at 662keV by far (fig 3a). Furthermore, a strong attenuation of pulse counts becomes visible towards the higher energies. In addition, an abrupt drop of pulse counts for energies below 25keV occurs. When the background measurement from 98h of spectrum accumulation inside of an empty lead shielding is compared to the spark gap tube measurement, a similar attenuation shape can be observed. And even when the background is subtracted, the corrected spectrum of a sample measurement still shows attenuation effects, a strong one towards the high energies and an abrupt one towards the low energies (fig. 3b).

The oversized spike at about 32keV (XRF of Cs137) and the distorted spectrum makes the manual or even automated identification of peaks and the analysis of the spectrum difficult and error prone. Therefore, postprocessing of the raw spectrum data with the goal of equalizing the shape of the spectrum towards what would be ideally expected is an option to improve peak identification and analysis. Different gain setting for adjacent energy bands that make up the overall energy range is a well-known approach for spectrum equalization. The Radiacode RC-101 used for the measurement shown in fig. 3, also offers a sliding-knob based simple equalization (Amplif) with the effect of successively amplyfing the count values towards the higher frequency bins. This may mitigate the distortion effect but does not completely avoid it (fig. 4).

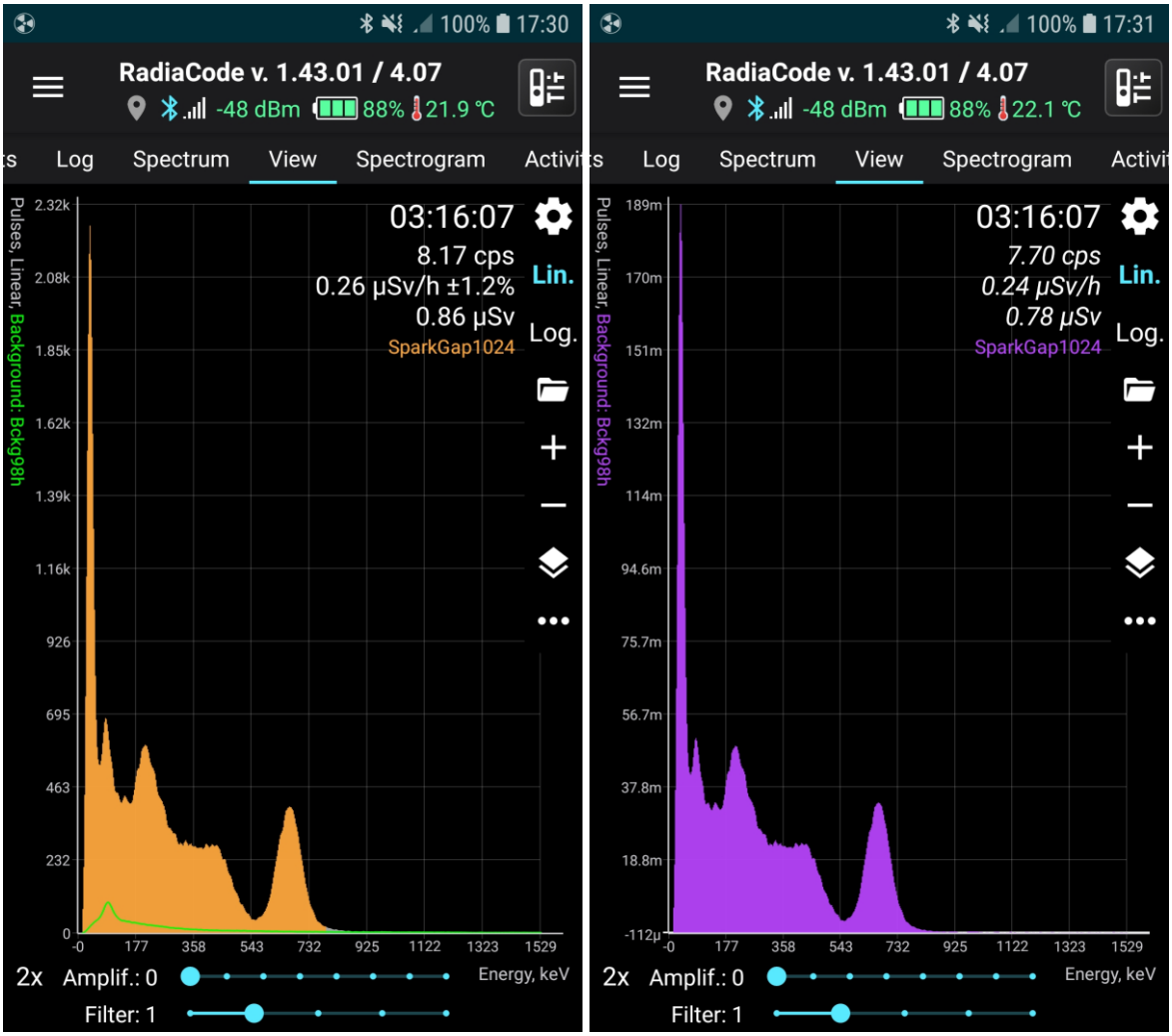


Fig. 3a (left): Measurement result of an old spark gap tube containing a small amount of Cs137 with a small handheld measurement device based on a 10x10x10mm CsI scintillation detector with SiPM /3/.

Fig. 3b (right): The same measurement as shown in fig. 3a but the background subtracted.

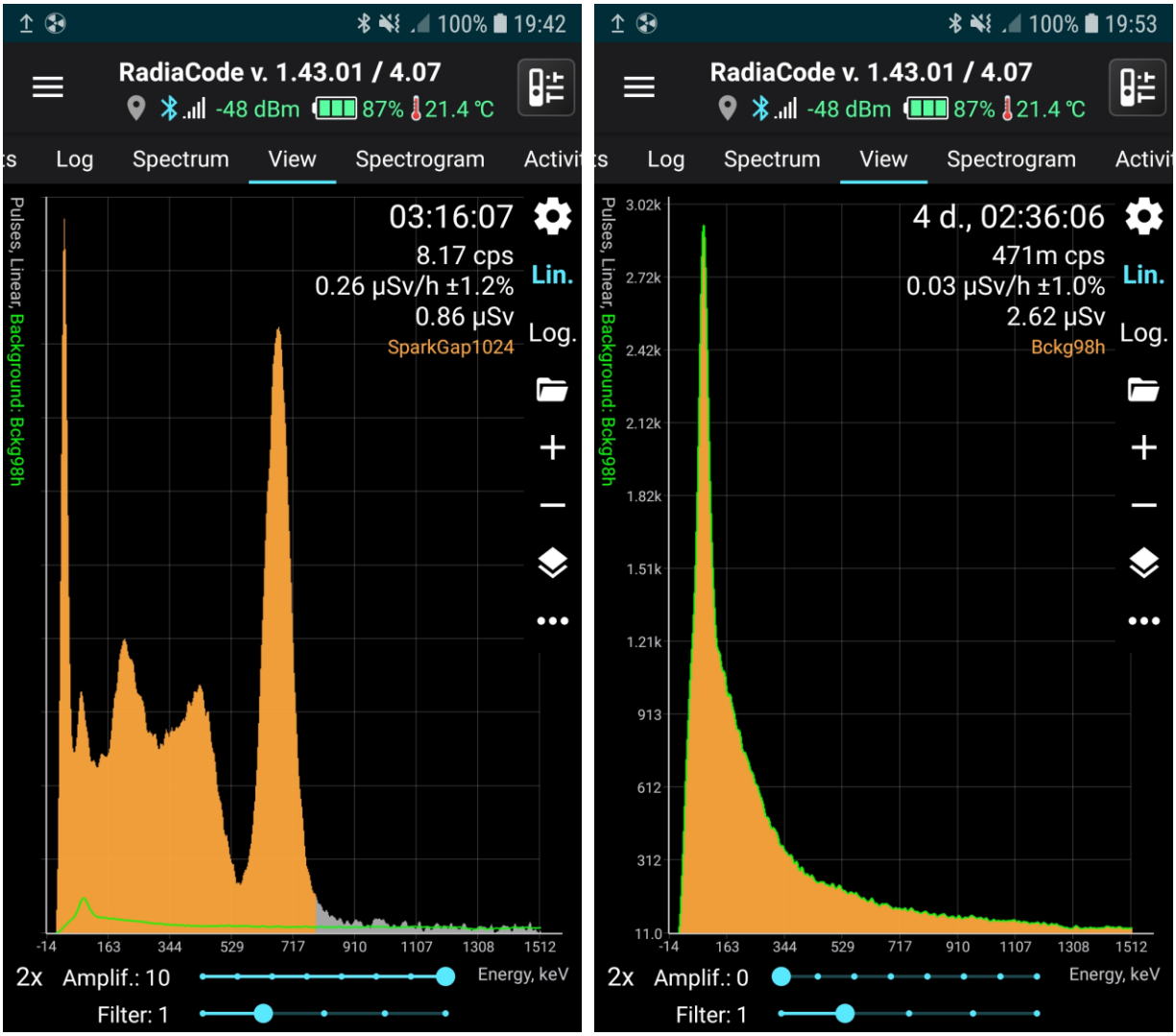

Fig. 3c: Amplif sliding knob applied to the data of fig. 3a

Fig 3d: Background measurement using the same lead shielding as for the measurement of the Cs containing spark gap tube

When analyzing the spectrum from the background measurement in fig. 3d, a major finding is the fact that the shape of the background function resembles a detector counting efficiency curve of a small size detector. The shaping of the background measurement may be attributed to the impact of the detector response to the ambient cosmic radiation that still penetrates the lead shielding. The much higher counting efficiency of the small crystal for the lower energies may outperform the higher absorption of the lower energy cosmic photons in the lead shielding by far and thus dominates the shape of the resulting spectrum. In case of additional detector internal radiation effects contribute to the resulting background spectrum they may also get shaped by the detector response function. In total, the detector response function has a significant and dominant influence on the shape of the background spectrum. This finding, however, suggests the use of the inverted shape of the background spectrum data for the equalization of the actual measurement data since the measured data will be shaped in a similar way. This idea of course is not based on a detailed physical understanding of how the background spectrum is generated. It simply represents a symptomatic equalization assuming that the background spectrum shape coarsely approximates the detector counting efficiency curve since the detector efficiency of a small detector massively influences the measurement of the background as well. Because the shape of the detector efficiency affects the actual measurement in the same way, a function extracted from the

approximating the background spectrum shape and taking the inverse of it, can be used as an equalization of the actual spectrum.

This finding leads to the proposed method and in turn to an algorithm implementable in software for postprocessing or in FW inside a measurement device. It can perform equalization of a spectrum accumulated from a small sized scintillation detector in an adaptive way. The method is adaptive in the sense of being able to consider the specific background conditions for a measurement and it is adaptive to the specific properties of the detector it is applied to. It is composed of the following steps:

1. Generation and storing of equalization parameters
1.1) Defining an analytical model for the shape of a background spectrum shape with a limited set of parameters for model- or curve-fitting, similar as for a detector efficiency
1.2) Measurement of a background spectrum
1.3) Fitting the model to the background spectrum shape by varying the parameters using a quality-of-fit metric
1.4) Storing the model parameters

2. Applying the equalization to a measurement
2.1) Multiplication of the measured data with the inverse of the background model data using the stored parameters and the parametrized model or alternatively dividing the measured data by the background model data
2.2) Normalization of the equalized data to either a peak maximum or any other reference point

As an example, an algorithm implementing the above-mentioned steps was written using Matlab (or respectively Octave) and was deployed for postprocessing the spectrum data exported from the Radiacode RC-101 as an example of a small-sized handheld gamma radiation measurement instrument.

In the first case, the method is applied to a Cs 137 spectrum measured from a spark gap tube as shown in fig 3a-d. The Cs 137 spectrum measured with the Radiacode RC-101 appears distorted by the small detector of the instrument and is equalized using the described method.

As a first step, an analytical model was defined following the typical approach for defining a model for the detector efficiency curve. The model has the form:

```
fitLin = exp(p(1)*logEnyR2.^2+p(2)*logEnyR2+p(3));
```

In this expression, p(1), p(2) and p(3) are the model parameters and logEnyR2 is the logarithm taken on the energy data after energy calibration was performed.

The curve fitting is performed with the Matlab function polyfit() that fits a polynomial of order n to a dataset minimizing the least mean square error. In this case the polynomial is of order 2. The variable logdPR2 represents the logarithm of the spectrum data at the energies logEnyR2. To perform this model fit, the background spectrum needs to be measured with the measurement instrument completely enclosed into lead without the radiation source for a sufficiently long time. The resulting background spectrum is shown in fig. 4.

The result of the model fit is the parameter array p with the 3 parameter elements p(1), p(2) and p(3).

```
p = polyfit(logEnyR2, logdPR2, 2);
```

To obtain a stable model however, the fit is restricted to a range selected such that the fit results in reasonable matching to the original background data. In this case the fit range is limited to the energies from 11keV to 500keV.

The model function fitLog that fits into the logarithm of this dataset (logEnyR2, logdPR2) can be created from the function polyval():

```
fitLog=polyval(p,logEnyR2);
```

Now, both functions, the model function fitLog and the logarithm of the data logdPR2 can be compared along the logarithm of the energies logEnyR2. Both functions are shown in fig. 5. The fitted model can then be translated back from the logarithmic domain into the linear domain and the resulting linearized fit can be represented along the energies for the whole range (fig. 6). This highlights that the model does not perfectly fit the original data set, since the model restricts to a polynomial of order 2. It becomes visible that the error of the model is largest at the sharp bending of the measured data towards the very low energies. A higher order polynomial would generate less error in this region but would cause oscillations at other regions. Therefore, the polynomial was kept as small as possible.

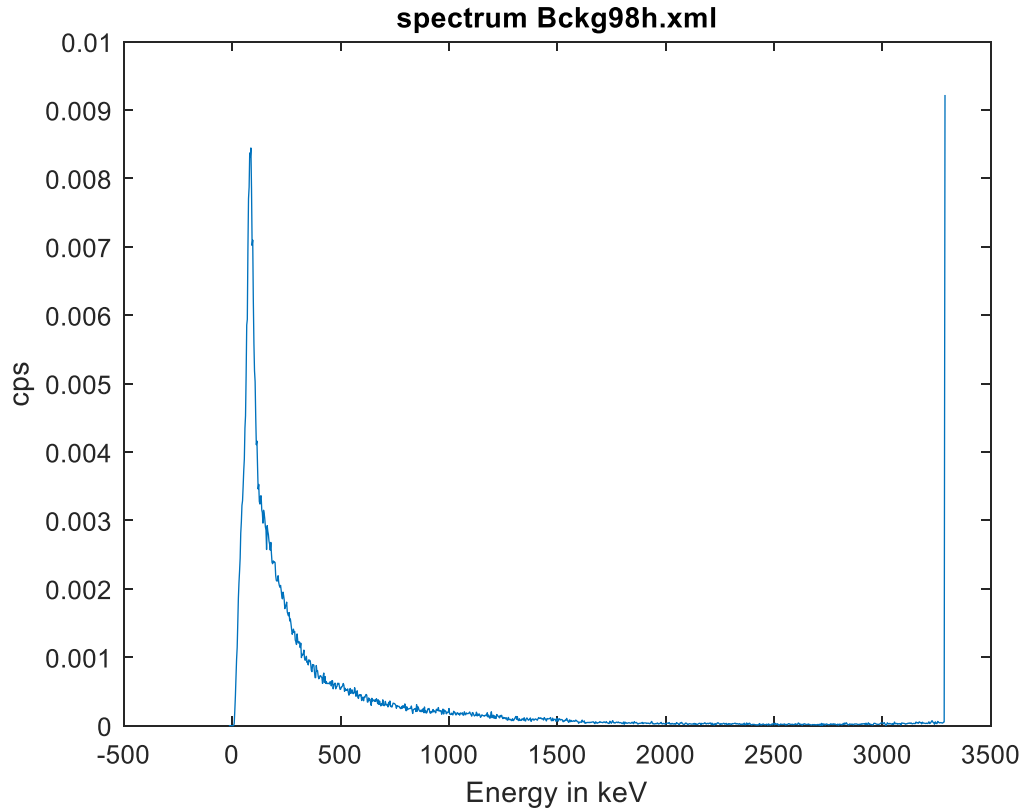


Fig 4: Raw spectrum data of the background as exported by the measurement instrument RC-101. The last spectrum bin is known to be incorrect in many cases for the current instrument firmware

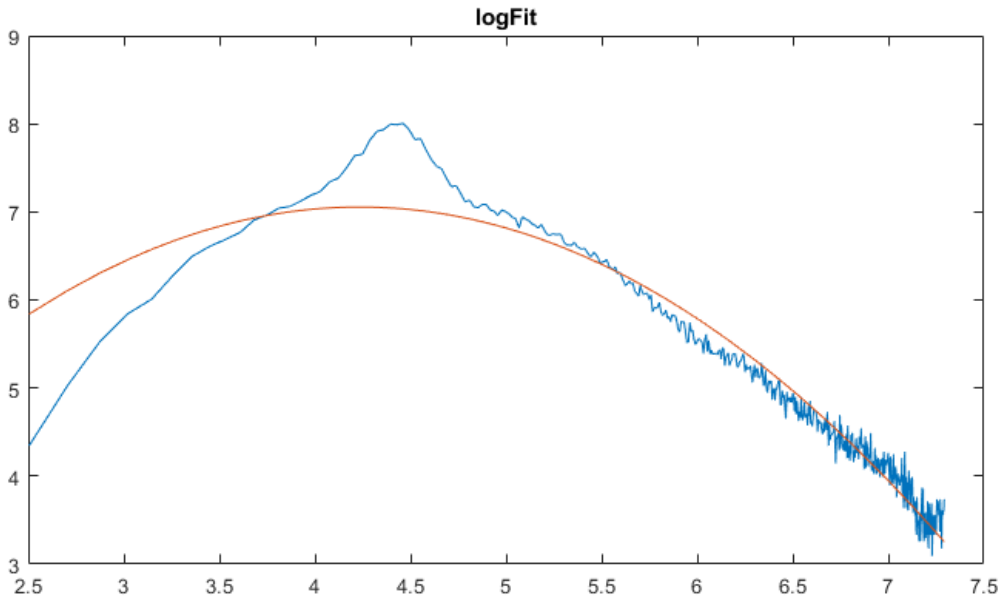


Fig. 5: A polynomial fit is performed on a data set the is the logarithm of the spectrum data versus the logarithm of the energy of the spectrum bins

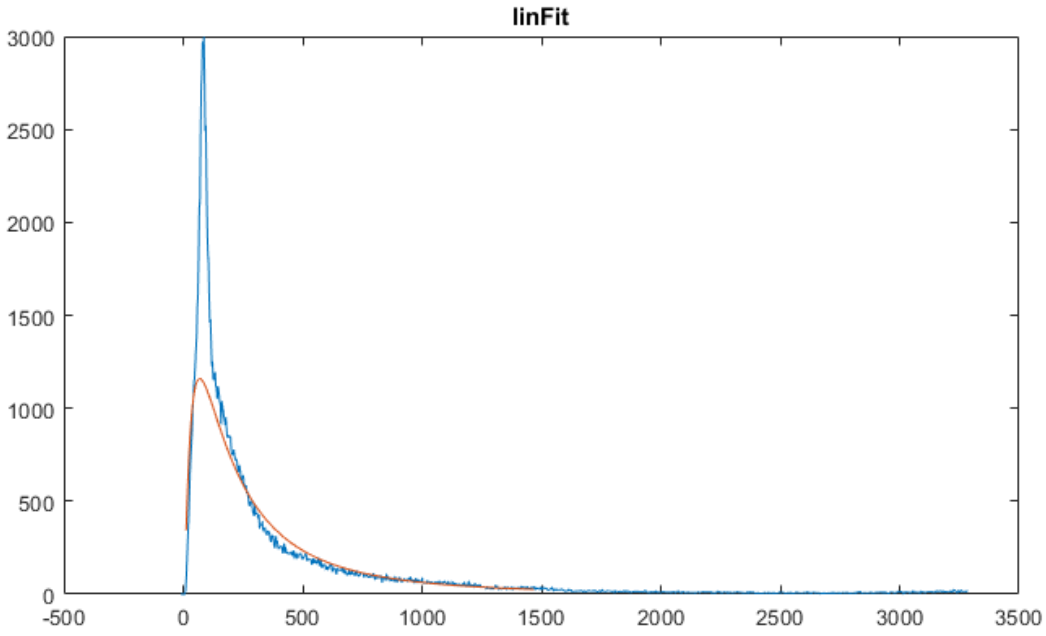


Fig. 6: The background model taken from the polynomial fit in comparison to the original background spectrum data

In the next step the inverted model is applied for equalization of the spark gap raw spectrum data as measured by the Radiacode RC-101 device. Fig. 7 shows the raw spectrum measurement data as exported from the Radiacode RC-101. It quickly can be recognized that the first spike is the XRF-peak from the Ba137m at 32keV that gets extremely overemphasized by the high sensitivity of the small CsI detector unit of the RC-101 measurement device. Compared to the XRF-peak, the actual photopeak of the cesium appears strongly attenuated. Applying the equalization with the inverse background model, however, returns a spectrum that looks much more reasonable. Fig. 8 shows an annotated graph of the compensated spectrum in which the different peaks now appear in a more realistic relationship with respect to their amplitudes.

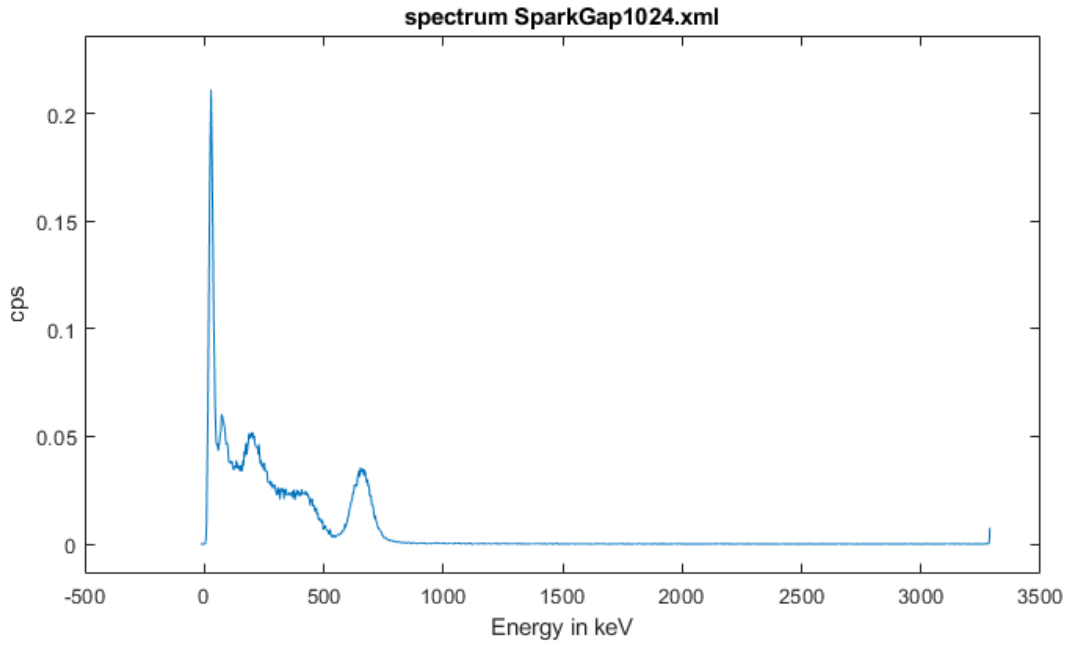


Fig. 7: The raw spectrum data from measuring a spark gap tube with Cs137 pre-ionization

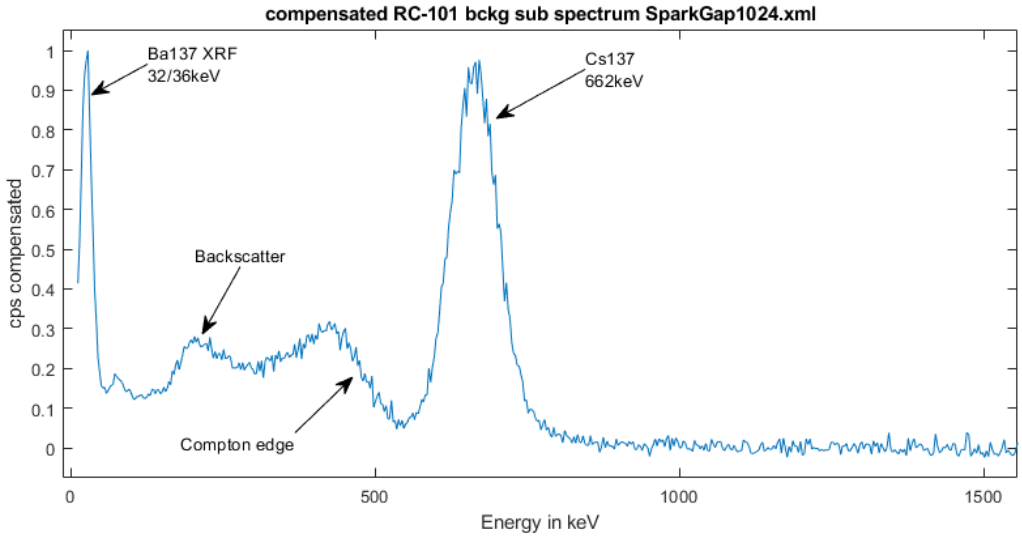


Fig. 8: The equalized spectrum measured from the spark gap tube

To demonstrate the method in an even more realistic case, contaminated soil taken from the embankment of the rainwater drainage system into a nearby ditch named “Hirschgraben” close to the nuclear research center formerly called “Kernforschungszentrum” in Karlsruhe, Germany was analyzed with the Radiacode RC-101. According to official reports, the soil contains 3800Bq/kg Cs137 and 487Bq/kg Am241 because of one or more former nuclear incidents. Whereas this amount of cesium can still be detected with a lower-cost consumer measurement instrument, the much smaller activity concentration of Am241 is challenging to detect. However, due to the small CsI detector geometry, the detector sensitivity of the Radiacode-101 is high close to 59keV, therefore it can easily detect the energy where Am241 emits its gamma radiation. Therefore, when measuring about 500g of soil in a lead castle, the Am241 peak appears extremely pronounced. In the raw spectrum data (fig. 9), the Am241 peak appears just following the XRF-Peak of the Ba137 and still can be separated from it.

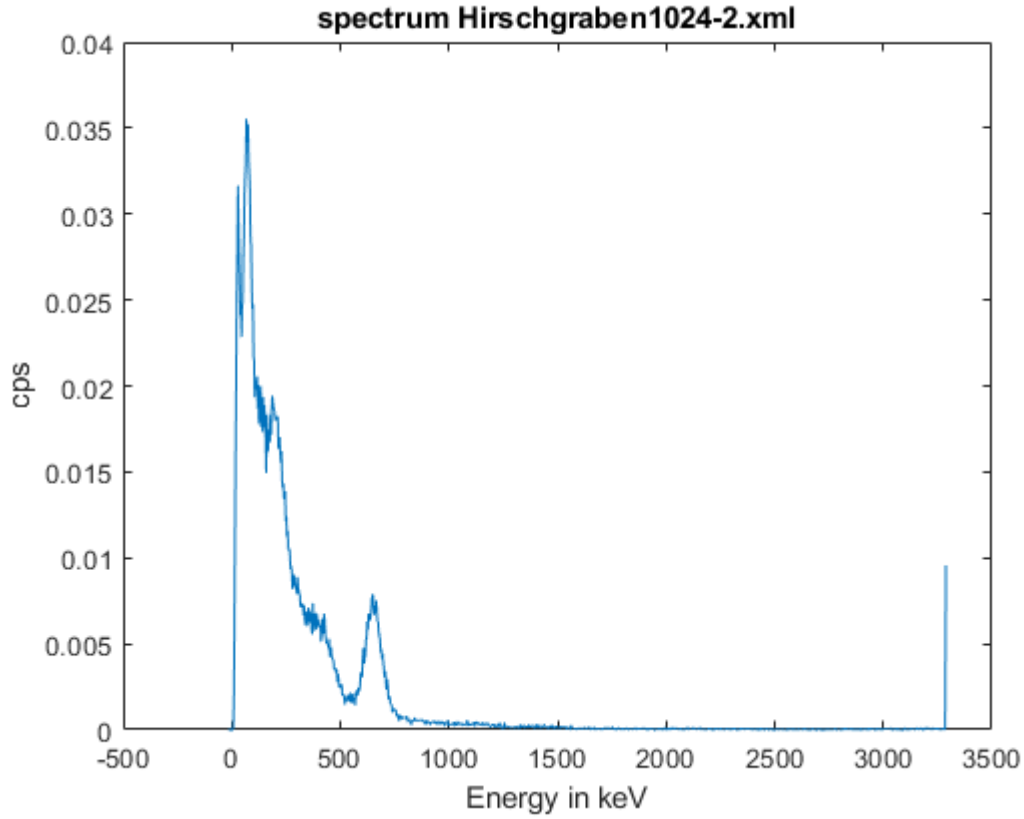


Fig. 9: The raw spectrum data from measuring a soil sample contaminated with Cs137 and Am241 taken from the embankment of a creek near the former Kernforschungszentrum Karlsruhe (KfK)

In the graph of fig. 10, the result of the equalization with the background function is shown in an annotated form. The ratios of the peaks become changed due to the compensation effect of the equalization. Again, this equalized representation appears much more reasonable with respect to the sizes of the peaks and the shape of the spectrum.

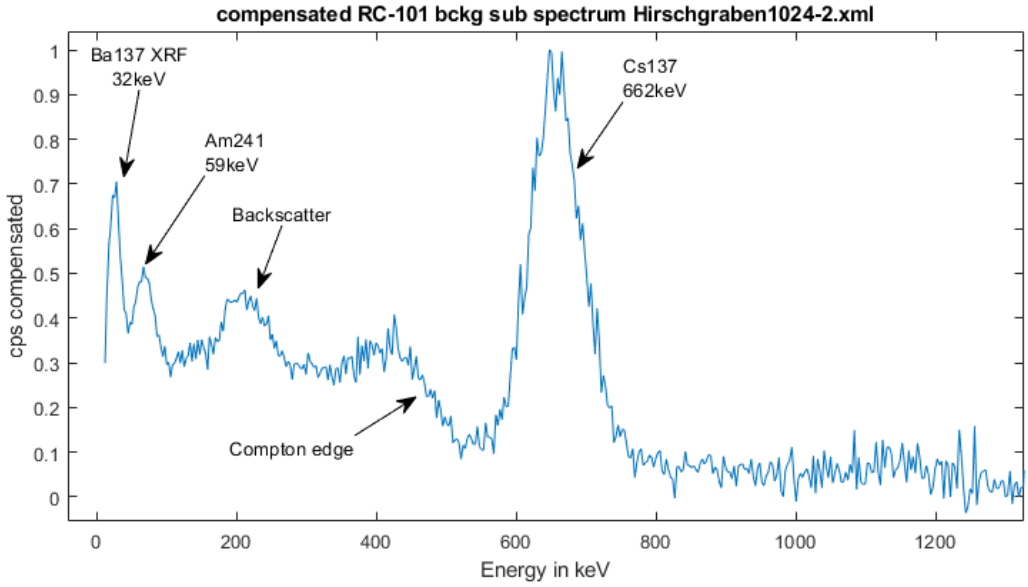


Fig. 10: The equalized spectrum measured from the contaminated soil sample

Finally, the method is demonstrated with an even more complex radiation source. Five thoriated tungsten electrodes for tungsten inert gas welding (TIG) are used. Due to the age of > 10 years, the thorium already formed daughter products from the thorium decay chain such as Ac228 and Tl208 that generate several distinct peaks in a gamma spectrum. The 5 electrodes were attached onto the body of the Radiacode RC-101 and a 20-hour spectrum was accumulated.


Fig. 11: Thoriated tungsten welding needles measured with the Radiacode RC-101 to obtain a more complex spectrum from Th232 and its daughter products

In a linear representation across the entire energy range the measurement device is specified for, a dominating peak at 67keV and a smaller peak at 283keV become visible that can be attributed to Pb212 in the Th232 decay chain. The rest of the spectrum just shows two more weak wiggles. A meaningful automated nuclide identification would be hardly possible this way.

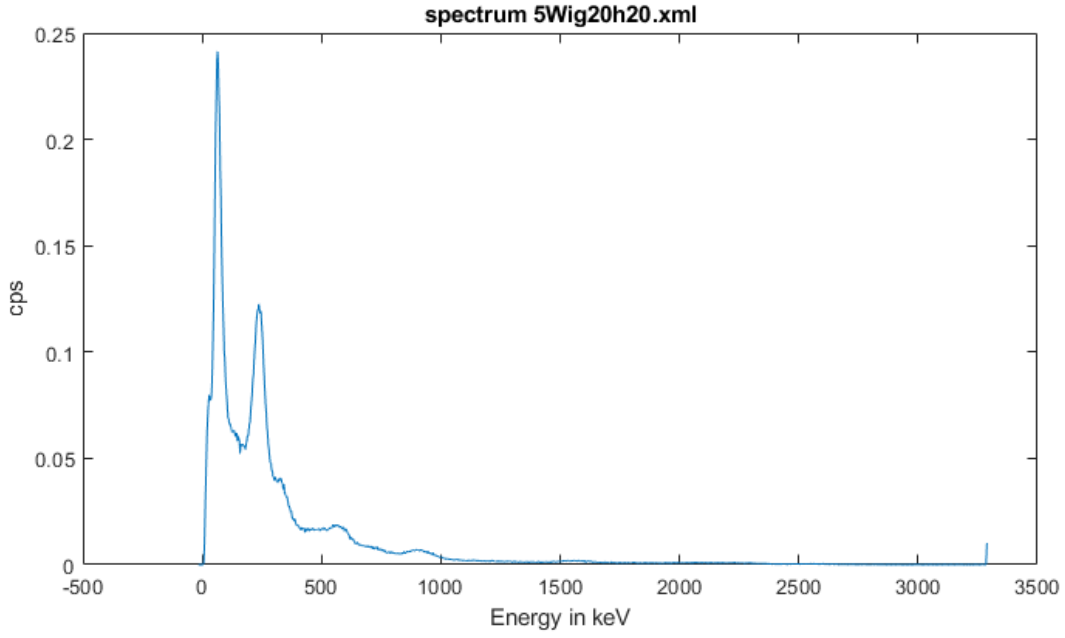


Fig. 12: The raw spectrum data from measuring 5 needles as used for tungsten inert gas welding (TIG)

In contrast, when the spectrum is equalized based on the inverse background function an assignment of the well-known peaks in the Th232 decay chain is easily possible, perhaps with one exception. The first peak at about 67keV was assigned to the XRF of tungsten but only with the a priori knowledge that the welding electrodes are made of tungsten that had been thoriated. The Th232 atoms in the thorium-wolfram alloy are in immediate vicinity to the tungsten atoms and are therefore able to excite the emission of characteristic X-rays (Kα and Kβ at 59 and 67keV). On the other hand, the tungsten also absorbs the particle emission of the Th232 and therefore attenuates the generation of the typical X-rays from the lead in the lead castle that normally is the case when the lead castle is not specifically shielded to prevent lead X-ray generation.

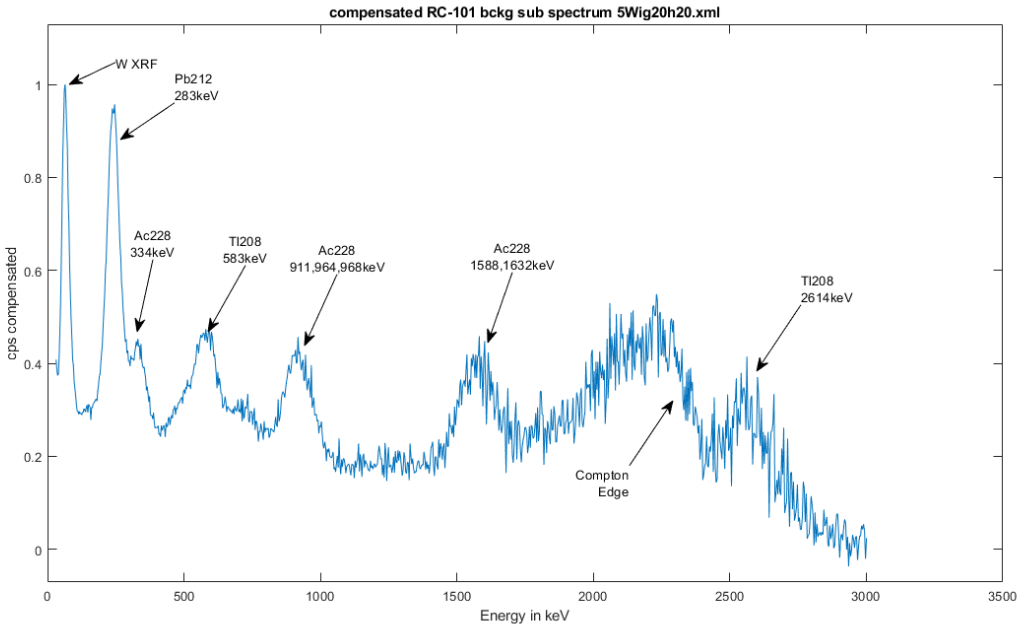


Fig. 13: The equalized spectrum generated from the measurement of the TIG welding needles

After equalization of the spectrum according to the presented method, the tungsten X-ray peak appears as the first peak in the spectrum in a more reasonable amplitude ratio compared to the Pb212 peak. Also, the higher energy peaks in the Th232 chain are now more adequately pronounced and easily allow nuclide identification. The Tl208 peak at 2614keV becomes clearly visible even though it was nearly invisible in the raw spectrum of the instrument, due to the very low count rate of the instrument at those energies.

As a conclusion, the proposed method of using the inverted data from a background measurement for equalization of spectrum data taken from measurement equipment using small sized scintillation detectors as it is described above, is clearly beneficial when the spectrum information needs to be postprocessed for e.g. (automated) nuclide identification or other purposes. It restores the shape of a distorted spectrum to a shape as it is expected from larger detectors. The successful application and functional implementation of a respective algorithm in Matlab is demonstrated in various cases. What still needs to be investigated is the error caused by the equalization compared to a spectrum from a large detector as well as the specific impact of the various sources responsible for the error.

**Literature**

/1/ Efficiency Calculations for Selected Scintillators; Saint-Gobain Crystals; 2018

/2/ Hyunwoong Choi; Experimental Investigation of the photo-peak detection efficiency of SiPM-based CsI(Tl) spectrometer with uncertainty calculation; Transactions of the Korean Nuclear Society Autumn Meeting Changwon, Korea, October 20-21, 2022

/3/ Detector of nuclear radiation and spectrometer Radiacode 102; Radiacode Ltd; radiacode.com

/4/ Bernd Laquai; Das KIT: Innen Hui und Außen Pfui – Das Karlsruher Referenz-Cäsium; 2021
http://www.opengeiger.de/GeigerCaching/KarlsruherReferenzcaesium.pdf

/5/ Lena Drieling; Radioökologische Untersuchung einer Altlast in Süddeutschland; Institut für Radioökologie und Strahlenschutz, Universität Hannover; 2022
https://www.irs.uni-hannover.de/fileadmin/irs/Arbeiten/Bachelor/bacdriel.pdf